

The Inhomogeneous Background of H₂ Dissociating Radiation During Cosmic Reionization

Kyungjin Ahn, Paul R. Shapiro, Ilian T. Iliev, Garrett Mellema & Ue-Li Pen

The first, self-consistent calculations of the cosmological H₂ dissociating UV background produced during the epoch of reionization (EOR) by the sources of reionization are presented. Large-scale radiative transfer simulations of reionization trace the impact of all the ionizing starlight on the IGM from all the sources in our simulation volume down to dwarf galaxies of mass $\sim 10^8 M_\odot$, identified by very high-resolution N-body simulations, including the self-regulating effect of IGM photoheating on dwarf galaxy formation. The UV continuum emitted below 13.6 eV by each source is then transferred through the same IGM, attenuated by atomic H Lyman series resonance lines, to predict the evolution of the inhomogeneous background in the Lyman-Werner band of H₂ between 11 and 13.6 eV.

1 Suppression of Minihalo Pop III Star Formation by H₂ Dissociating UV Background

- 1 Simulations suggest first stars formed inside minihalos of mass $M \sim 10^6 M_\odot$ at $z \gtrsim 20$, when H₂ cooled the primordial, metal-free halo gas and gravitational collapse ensued.
- 2 H₂ Lyman-Werner (LW) band photons ($\sim 11 - 13.6$ eV) dissociate H₂: Too much LW background [intensity $J_{\text{LW}} > (J_{\text{LW}})_{\text{threshold}}$] \rightarrow first star formation suppressed.
- 3 Earlier estimates (Haiman et al 2000) found that sources of reionization made $J_{\text{LW}} > (J_{\text{LW}})_{\text{threshold}}$ long before reionization is complete \rightarrow minihalos sterilized before they could contribute significant reionization.
- 4 Previous calculations: cosmic mean LW background by a homogeneous universe approximation. Sources and IGM uniformly distributed, with uniform emissivity given either by analytical approximation (Haiman et al. 2000) or by sum over sources found in small-box simulations, too small to account for large-scale clustering of sources or follow global reionization (e.g. Ricotti et al. 2002; Yoshida et al. 2003)
- 5 Here we present the first self-consistent radiative transfer calculations of the **inhomogeneous LW background** produced by the same sources which reionized the universe in a large-scale radiative transfer simulation of reionization.

2 The First Self-Consistent Calculation of the Inhomogeneous LW Dissociating Background during Epoch of Reionization (EOR)

1 Computational Challenge

- The horizon for seeing LW photons is ~ 100 comoving Mpc (hereafter, “cMpc”), much larger than the size of typical HII regions (\sim a few ~ 10 cMpc).
- The mean free path for LW photons (~ 100 cMpc) is much larger than mean free path for H ionizing photons. \rightarrow Need to account for sources distributed over large volume and look-back time.
- LW band photons redshift and get attenuated by H atom Lyman series resonance lines. Need to perform multi-frequency radiative transfer from each source in cosmological volume ($\gtrsim (100 \text{ cMpc})^3$), which is computationally VERY expensive. Can we overcome this difficulty? \rightarrow YES, with precomputed “picket-fence” modulation factor, to alleviate frequency sampling, as described below.

2 Method (Fast and Accurate)

- **“picket-fence” modulation:** attenuation of LW photons from a single source. As a LW band photon travels, when its frequency redshifts into an H resonance line, it is absorbed and some fraction turn into low frequency photons. If it resonantly scatters, it is quickly reabsorbed, until all resonant photons turn into low frequency photons below LW bands. For homogeneous universe, this gives “saw-tooth” modulation of the spectrum. But in inhomogeneous universe, this treatment is not valid. Each source at z_s is attenuated by its own “picket-fence” modulation, which is a function of r_{cMpc} (comoving distance from source to observer at z_{obs}), as described below. $r_{\text{cMpc}} = 2cH_0^{-1} \Omega^{-0.5} [(1+z_{\text{obs}})^{-0.5} - (1+z_s)^{-0.5}]$.

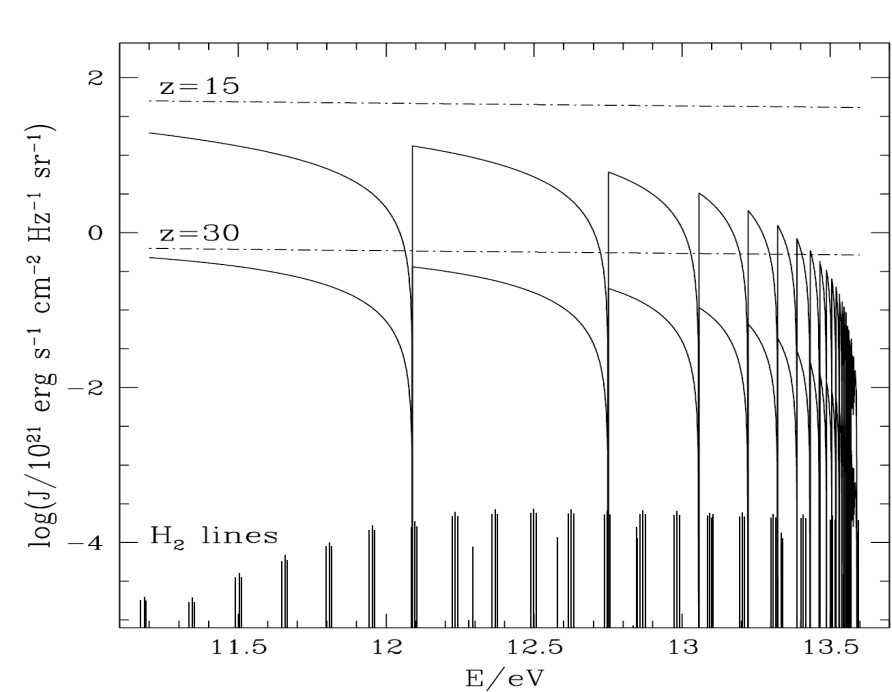


Fig 1. Illustrative spectrum of the UV background at redshifts $z=30$ and $z=15$ in a homogeneous universe, calculated by Haiman, Abel & Rees (2000). The solid lines show the spectrum after attenuation by neutral H in the high-redshift IGM; dashed lines show the spectrum without this absorption. For reference, at the bottom of the figure, the location of the 76 LW lines of H₂ is shown. The length of each line indicates its relative contribution to dissociations of H₂.

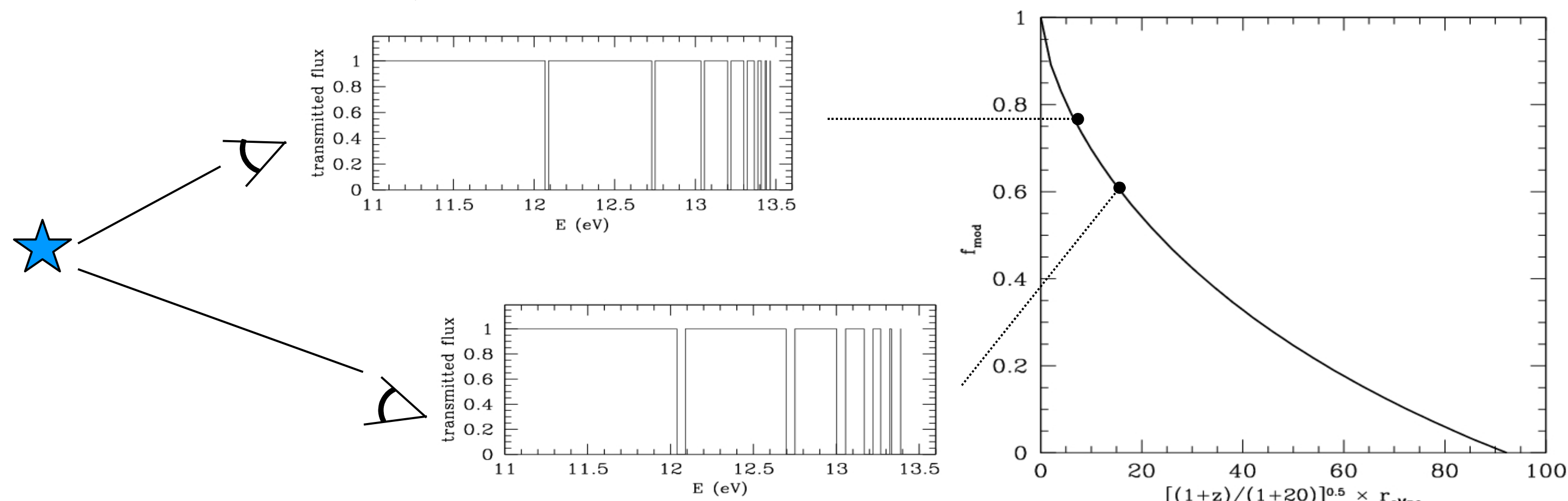


Fig 2. “picket-fence” modulation. A source observed at different distances suffers different amounts of attenuation, dilution, and redshift. As continuum (flat-spectrum assumed) photons redshift, all the photons which have redshifted to H atom resonance lines are turned into low-energy photons. This leaves gaps in observed spectrum, which depend on the distance to the source. The modulation factor (right panel) is the effective transmission rate, which drops as the distance increases, until source is completely attenuated at $r_{\text{cMpc}} = 92 [(1+z)/21]^{-0.5}$. With this modulation factor, we are able to compute LW intensity without costly multi-band calculation.

- **Retarded time effect:** Construct a conformal spacetime diagram, then choose an observing point (in space and time). Draw a past light-cone and add up contributions from all sources whose world lines cross the light-cone.

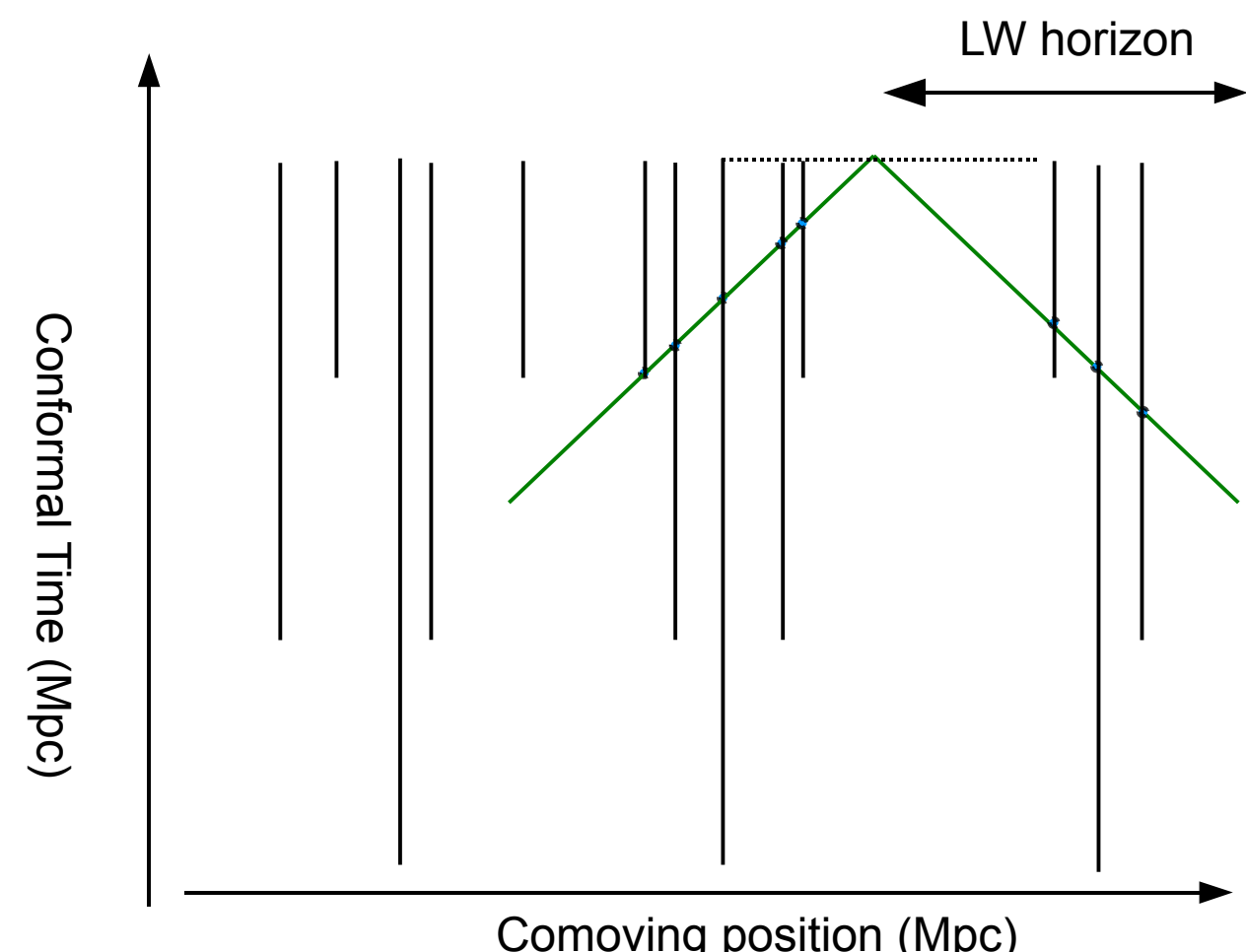


Fig 3. Conformal spacetime diagram, to be used to calculate source contribution from cosmological distances. Each source contributes LW flux of $f_{\text{mod}} \cdot L/D^2$, where L is luminosity, D is the luminosity distance to the source, and f_{mod} is the picket-fence modulation factor which accounts for IGM opacity. This scheme naturally accounts for the finite light-crossing time of radiation.

3 Inhomogeneous LW Background: Inhomogeneous Feedback Effect on the Formation of the First Stars inside Minihalos

1 Illustrative EOR simulation (Self-Regulated: Iliev et al. 2007; case f2000_250S)

- Radiative transfer sim (203^3 cells) thru N-body sim (1624^3 particles, 3248^3 cells) density field, ionized by all halos $M/M_\odot > 10^8$ in $(50 \text{ cMpc})^3$ volume: covers all atomic cooling halos.
- Formation of sources inside small-mass halos ($10^8 < M/M_\odot < 10^9$) is suppressed if H II regions overtake their formation sites. Pop III high efficiency emitters with top-heavy IMF are assumed, with $f_v = f$, $f_{\text{esc}} N_i = 2000$, and with $N_i/N_{\text{diss}} \sim 15$ (f = star formation efficiency; f_{esc} = ionizing photon escape fraction; N_i = number of ionizing photons emitted per baryon; N_{diss} = number of H₂ dissociating photons emitted per baryon)
- Formation of sources inside large-mass halos ($M > 10^9 M_\odot$) are not suppressed even inside HII regions. Pop II low efficiency emitters with Salpeter IMF are assumed, with $f_v = f$, $f_{\text{esc}} N_i = 250$, and with $N_i/N_{\text{diss}} \sim 1$

2 Mean H Ionizing background and H₂ dissociating background by atomic cooling halos

- Small-mass ($10^8 < M/M_\odot < 10^9$) halos are suppressed before contributing too many ionizing photons \rightarrow Reionization is finished by large-mass ($M > 10^9 M_\odot$) halos
- Accordingly, initial LW intensity (J_{21}) is dominated by small mass halo contribution, while at later epoch by large-mass halo contribution.
- If reionization source properties are different from our illustrative case, especially in f_{esc} and N_i/N_{diss} , the same global ionization fraction $\langle x \rangle$ would not mean the same J_{21} !

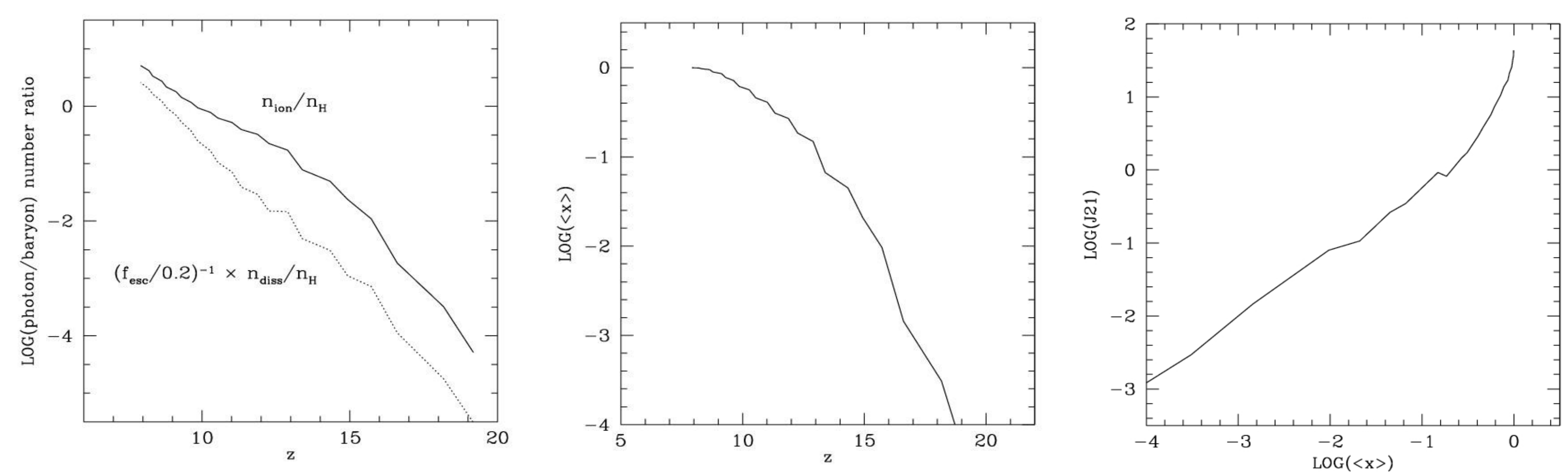


Fig 4. Global history of cosmic reionization and LW intensity evolution. (Left): The accumulated number of ionizing photons per baryon VS. the number of dissociating photons per baryon. (Middle): Global evolution of ionization fraction $\langle x \rangle$. (Right): Global evolution of LW intensity J_{21} ($= J_v / 10^{21} \text{ erg cm}^{-2} \text{ s}^{-1} \text{ Hz}^{-1} \text{ sr}^{-1}$). Note that if reionization source properties change, especially in ionizing photon escape fraction (f_{esc}) and ratio of dissociating/ionizing photons, J_{21} may differ even at the same global ionized fraction.

3 Inhomogeneous LW background is apparent, with fluctuation scale of a few - ~ 10 cMpc. This will induce an inhomogeneous LW feedback, hence inhomogeneous minihalo star formation rate. The most pristine environment + the most active minihalo star formation activity will occur where LW intensity is the smallest, as shown below.

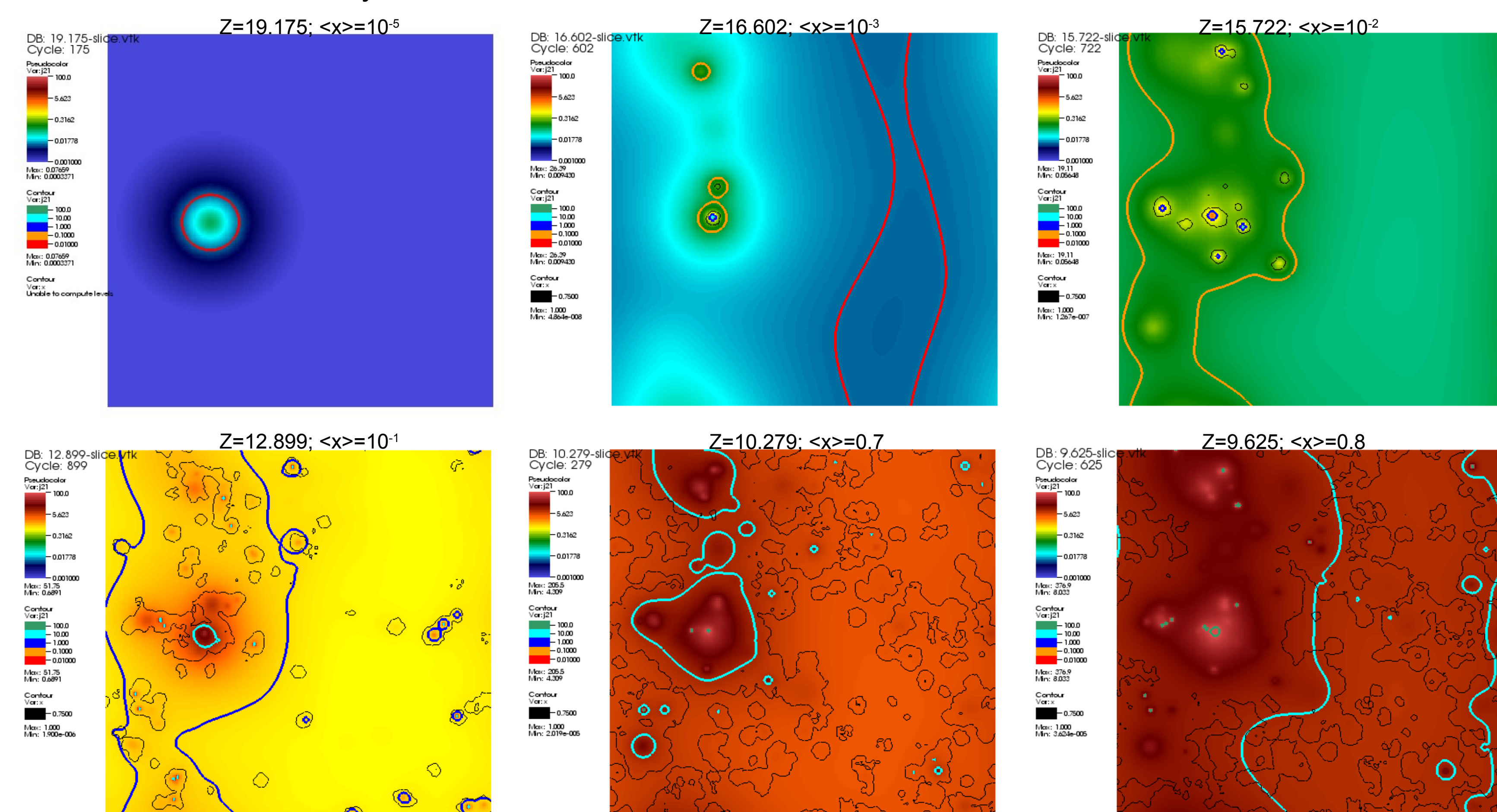


Fig 5. Patchy reionization and patchy H₂ dissociating background in $(50 \text{ cMpc})^3$ box. Contours of thick colored lines represent different J_{21} contours (red $J_{21} = 0.01$; orange = 0.1; blue = 1; cyan = 10; green = 100), and the black contours represent the ionization fronts. J_{21} contours grow rapidly and overlap at each level. Minihalos are subject to spatially-varying LW feedback effect, thus yielding spatially-varying minihalo star formation rate. JWST may be able to detect clustered minihalo population at $z \gtrsim 15$ in regions of least LW feedback.

REFERENCES

- Haiman, Z., Abel, T., & Rees, M. 2000, *ApJ*, 534, 11
- Iliev, I. T., Mellema, G., Shapiro, P. R., & Pen, U. L. 2007, *MNRAS*, 376, 534
- Ricotti, M., Gnedin, N. Y., & Shull, J. M. 2002, *ApJ*, 575, 33
- Yoshida, N., Abel, T., Hernquist, L., & Sugiyama, N. 2003, *ApJ*, 592, 645